Synthesis of Character Behaviour by Dynamic Interaction of Synergies Learned from Motion Capture Data

Aee-Ni Park[1], Albert Mukovskiy[1], Lars Omlor[1], Martin A. Giese[1,2]

[1]Lab. for Action Representation and Learning, Dept. of Cognitive Neurology,
Hertie Institute for Clinical Brain Research, Tübingen, Germany

[2]School of Psychology, University of Bangor, UK

Email: aee-ni.park@medizin.uni-tuebingen.de, martin.giese@uni-tuebingen.de

ABSTRACT

Character animation ideally combines the competing requirements of high realism and flexible automatic generation of behaviour. A method for real-time human character animation is presented, which self-organizes character behaviour with high degrees of realism by dynamic coupling of 'synergies' that are learned from motion capture data. Based on a new algorithm for blind source separation that considers time delays, highly compact generative models of body movements are learned from motion capture data. The learned components are mapped onto stable solutions of dynamical systems applying kernel methods, resulting in a coupled network of dynamic pattern generators whose state can be updated in real-time. This new framework is applied for crowd animation and the automatic generation of interactive behaviour for multiple characters.

Keywords: character animation, example-based motion synthesis, synergies, blind source separation, dynamical systems, motion blending.

1 INTRODUCTION

A core problem of modern computer animation is to accomplish high degrees of realism and flexibility at the same time. Animation based on motion capture data offers high levels of realism, but requires tedious editing of the recorded movements to adapt them to relevant constraints of the animation. On the other side, physics-based animation offers the possibility to build real-time capable animation systems that are able to self-organize character behaviour in a reactive manner, taking into account the behaviour of the user and other agents in the scene. However, such reactive systems for animation often produce simplified movements, lacking the rich details of realistic human body movement. It is an important challenge to develop systems that combine the advantages of these two approaches, exploiting motion capture data to simulate highly realistic human movements in a framework that is capable of the self-organization of interactive behaviour.

Motion Capture is presently the standard approach for the generation of highly realistic human movements. The recorded trajectories are typically retargeted to kinematical or physical models [e.g. Gle98a] and different methods for the editing and blending of motion capture data have been proposed [e.g. Wit95a; Ros96a]. Some recent algorithms concatenate segments of motion capture data automatically from large data bases, generating long animation sequences that fulfil specific boundary conditions [e.g. Gle03b; Ari03a; Saf04a]. Few recent studies have started to embed motion capture data into real-time capable animation systems [Hsu05a; Cha05a].

Another set of approaches in computer animation generates reactive behaviour of characters based on physical or dynamical models [e.g. Grz98a; Sha05a]. Many studies have focused on the simulation of scenes with many agents or crowds [e.g. Ulic02a], navigating autonomously or showing collective behaviours. The underlying character models are often strongly simplified, resulting in a manageable complexity of the system dynamics and dynamics simulation, but lacking subtle details of realistic human body movements. Some approaches have managed to simulate highly realistic human behaviour using dynamic models using sophisticated hierarchical control architectures [Sha05a; Hod95a]. However, the design of such systems is complex and the adjustment of their parameters requires much expertise of the animator. It seems thus interesting to develop simpler dynamical architectures that, however, can simulate complex human movements by integrating information learned by motion capture without the necessity of a detailed simulation of the human body dynamics.

We present a new approach that combines accurate simulation of human movements exploiting motion capture data with real-time simulation of reactive movements. By unsupervised learning, we construct highly compact trajectory models from motion capture data that depend only on a small number of hidden source signals. Behaviour is self-organized by low-dimensional nonlinear dynamical systems, whose state space is mapped onto the source signals exploiting kernel methods from machine learning.

This proposed approach is biologically inspired: In motor control it has been a classical concept that complex motor behaviour might be modelled by the superposition of simpler components ('synergies'), encompassing only a subset of available degrees of freedom and forming the basic units of control [Ber67a; Fla05a]. Recent studies in motor control have successfully identified such components applying unsupervised learning methods to trajectories or EMG signals [d'Av05a; Iva04a]. Opposed to standard methods, like PCA or ICA that require often 8-12 components to accomplish highly accurate approximations of human body movements [Saf04a], the proposed novel algorithm achieves the same accuracy with less components. Each learned component is then assigned to a dynamical system (similar to a 'central pattern generator') that generates its dynamics in real time. By coupling of the dynamical systems that drive the different components coordinated behaviour between different sets of degrees of freedom is accomplished. In addition, the dynamical systems are modulated by external forces, induced either by other agents in the scene or by user specifications.

The contributions of this paper are as follows: (1) Presentation of a new algorithm for the unsupervised learning of highly compact models from sets of trajectory data that are based on synergies; (2) development of a kernel-based method for the mapping of the extracted synergies onto nonlinear dynamical systems with defined stability properties; (3) a demonstration of this novel approach for a number of example scenarios from character animation.

In the following, we briefly describe the algorithm for the unsupervised learning of synergies from motion capture data (Section 2). We then discuss how such trajectory models can be linked to nonlinear dynamical systems, suitable for the simulation of trajectories in real-time (Section 3). We demonstrate how meaningful interactions between multiple avatars can be implemented by coupling such dynamical systems, and how autonomous navigation of the characters can be realized within this framework (Section 4). Finally, we discuss applications that illustrate the capabilities of this novel framework in Section 5.

2 SYNERGY-BASED TRAJECTORY MODEL

2.1 Motion capture data

Motion data were recorded using a VICON 612 Motion Capture System with 8 cameras and 41 reflecting markers, with a sample frequency of 120 Hz. The animations presented in this paper are based on two data sets of gaits. The first contains straight walking with neutral and different emotional styles (sad, happy, angry, fearful). The second data set includes neutral and emotional straight walking and neutral walking along a circular paths (with rotations of 45 deg left or right per double step).

The recorded position trajectories were fitted with a hierarchical kinematical model (skeleton) consisting of 17 joints. Rotations between adjacent segments were parameterized as quaternions. The angles given in an axis angle representation served as basis for the modeling by unsupervised learning.

2.2 Blind Source Separation

Joint angle trajectories $x_i(t)$, after substracting the means, were approximated by a weighted mixture of source signals. As analyzed in detail in [Oml07a], a very compact model for gait trajectories is obtained by fitting an overdetermined anechoic mixture model, e.g. a model with more data points than sources. Such a model is given by the equation:

$$x_i(t) = \sum_j w_{ij} s_j(t - \tau_{ij}) \qquad (1)$$

The functions $s_j(t)$ denote hidden source signals and the parameters w_{ij} are the mixing weights. Contrasting with common blind source separation techniques, e.g. PCA or ICA, this mixing model allows for time shifts τ_{ij} of the sources before linear superposition. Time shifts (delays), source signals and mixing weights are determined by the blind source separation algorithm described below. Detailed comparisons for periodic and non periodic trajectory data shows that the model (1) results in more compact trajectory approximations for human movement data, requiring less source terms than models based on standard PCA, ICA or Fourier series for the same level o accuracy [Oml06b].

Classical applications in acoustics for anechoic demixing assume frequently an under-determined mixing model of the form (1). A new algorithm for the solution of over-determined problems can be derived based on the Wigner-Ville transform [Mat03a]. The Wigner-Ville spectrum (WVS) of a random process x is defined by the partial Fourier transform of the symmetric autocorrelation function of x:

$$W_x(t, \omega) := \int E\left\{x(t + \frac{\tau}{2})\overline{x(t - \frac{\tau}{2})}\right\} e^{-2\pi i \omega \tau} d\tau \qquad (2)$$

Applying this integral transform to equation (1) results in the equation

$$W_x(t, \omega) := \sum_j {w_{ij}}^2 W_{sj}(t - \tau_{ij}, \omega) \qquad (3)$$

under the assumption that the sources are statistically independent. As two dimensional representation of one dimensional signals, this equation is redundant and can be solved by computing a set of projections onto lower dimensional spaces that specify the same information as the original problem. See [Oml06a] for further details.

For the described data set the estimated time delays vary only significantly between the joints, but not as a function of the emotional style. We thus constrained the joint angles to small intervals around the mean angle for each joint to remove ambiguities in the estimations of the delays. Also the obtained source functions were highly similar between different emotions and movement directions. We thus estimated a common set of source functions for the whole data set. Three source functions were sufficient to obtain a highly accurate approximation of the joint trajectories (accuracy > 96 % of the variance). Since source functions and delays were joint-specific, but identical over the whole data set, all information about emotion style and walking direction was encoded in the mixing weights w_{ij}.

3 DYNAMICS FOR REAL-TIME ANIMATION

The proposed trajectory model parameterizes high-dimensional trajectories in terms of a small number of basis signals. However, this representation is not suitable for real-time animation, e.g. for computer games. To make the system real-time capable, we established a mapping between the solutions of simple dynamical systems and source signals of the trajectory representation. The complete trajectory is then generated by a set of such simple dynamical systems, which are coupled to ensure temporal coordination of the different sources. In an abstract sense, the resulting system is similar to a set of coupled 'central pattern generators' in a biological system. Such architectures have been proposed as model for the generation of gaits and other motor patterns [Ijs02a; Sch03a].

In the following, we first introduce the attractor dynamics and discuss how the mapping between its solutions and the source signals of the trajectory representation is learned. Finally, we demonstrate how dynamic couplings can be introduced that stabilize the coordination within single characters, and which are suitable for the simulation of coordinated behaviour of multiple avatars.

3.1 Attractor dynamics

Often, behaviour can be mapped onto stable solutions of dynamical systems [Kel95a]. This has been successfully demonstrated in a variety of applications in robotics [e.g. Sch95a; Sch03a]. While our approach generalizes for non-periodic movements, for the experiments in this paper we simulated only periodic gaits. It seems a natural to choose limit cycle oscillators as dynamics for the generation of such periodic behaviours [e.g. Ijs02a; Sch03a]. Because of its well-studied dynamics, we use a Van der Pol oscillator as basis element of our architecture. This oscillator can be understood as a harmonic oscillator with amplitude-dependent damping. Its dynamics is given by the differential equation:

$$\ddot{y}(t) + \lambda \left(y(t)^2 - k \right) \dot{y}(t) + \omega_0^2 y(t) = 0 \qquad (4)$$

The parameter ω_0 determines the eigenfrequency of the oscillator, and the positive parameter k the amplitude of the stable limit cycle with a speed that depend on the positive parameter λ. After perturbations the state will thus return to this attractor. In addition, the structure of the dynamics does not fundamentally change for moderate couplings with other system components (structural stability). For more details see [And87a]. For each of the three source signals in the model (1) we introduce a separate Van der Pol oscillator.

3.2 Mapping of phase space onto source signals

The mapping between the phase space of the limit cycle oscillator and the values of the source signals is learned by Support Vector Regression (SVR) [Vap98a]. To avoid additional delays in the implementation, we introduce new signals for the individual sources with different delays according to the relationship:

$$\tilde{s}_{ij}(t) = s_j(t - \tau_{ij}) \qquad (5)$$

For each of these modified source signals we construct a separate mapping from the phase space of the Van der Pol oscillator that corresponds to the source s_j, which is given by the variable pair $\mathbf{y}_j(t) = [y_j(t), \dot{y}_j(t)]$ and the values of the variables $\tilde{s}_{ij}(t)$. This mapping is given by the nonlinear functions:

$$\tilde{s}_{ij}(t) = f_{ij}\left(\mathbf{y}_j(t)\right) \qquad (6)$$

The nonlinear function f_{ij} is learned by SVR from M training data pairs $\left\{\mathbf{y}_j(t_l), \tilde{s}_{ij}(t_l)\right\}_{1 \le l \le M}$ that are derived by sampling one cycle of the stationary solution of the oscillator and the modified source signal equidistantly over time. After the functions f_{ij} have been learned, the dynamics corresponds to three limit cycle oscillators with nonlinear instantaneous observers that map the state of each oscillator onto the corresponding set of delayed source signals. These signals then are linearly combined according to (7). The complete reconstruction of the joint angle trajectories requires the addition of the average joint angles m_i, which have subtracted from the data before the blind source separation (Figure 1):

$$x_i(t) = m_i + \sum_j w_{ij} \tilde{s}_{ij}(t) \qquad (7)$$

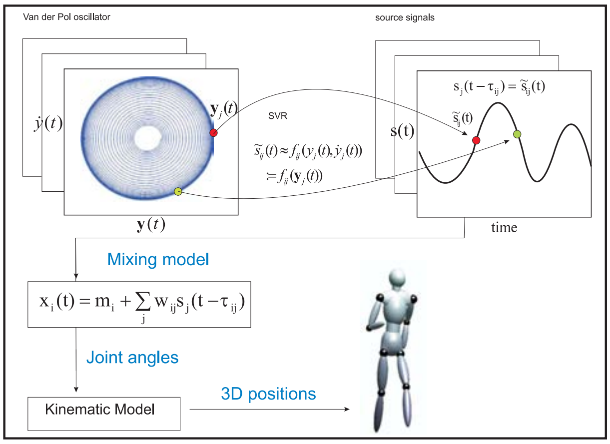

Figure 1: Illustration of the dynamics for real-time animation. The phase space of the limit cycle oscillator is mapped onto the time-shifted source signals using Support Vector Regression. Joint angles are synthesized by combining the signals linearly according to the learned mixture model (1). A kinematic model converts the joint angles into 3-D positions for animation.

3.3 Dynamic coupling

In order to stabilize the timing-relationship between the different sources ('synergies') we introduced dynamic couplings between the three oscillators that drive the source signals of the same avatar.

It has been shown applying contraction theory that stable behaviour of such oscillator networks can be accomplished by introduction velocity couplings [Wan05a]. The couplings within the same avatar were given in the form (cf. Figure 2):

$$\begin{aligned}
\ddot{y}_1 + \lambda\left(y_1^2 - k\right)\dot{y}_1 + \omega_0^2 y_1 &= \\
&\alpha\left(\dot{y}_2 - \dot{y}_1\right) + \alpha\left(\dot{y}_3 - \dot{y}_1\right) \\
\ddot{y}_2 + \lambda\left(y_2^2 - k\right)\dot{y}_2 + \omega_0^2 y_2 &= \\
&\alpha\left(\dot{y}_1 - \dot{y}_2\right) + \alpha\left(\dot{y}_3 - \dot{y}_2\right) \\
\ddot{y}_3 + \lambda\left(y_3^2 - k\right)\dot{y}_3 + \omega_0^2 y_3 &= \\
&\alpha\left(\dot{y}_1 - \dot{y}_3\right) + \alpha\left(\dot{y}_2 - \dot{y}_3\right)
\end{aligned} \tag{8}$$

Such dynamic couplings can also be exploited for simulating coordinated behaviour of multiple characters and crowds, for example, to enforce that multiple avatars walk in synchrony (e.g. soldiers in lock-step). To implement such couplings we only connected the oscillators assigned to the source with the lowest frequencies (Oc1). Introducing unidirectional couplings it is possible to make multiple characters following one, who is the leader [Wan05a].

3.4 Interactive change of motion style

The proposed model for the real-time generation of trajectories permits style morphing in a straight forward way. To interpolate, e.g., between neutral (style a) and

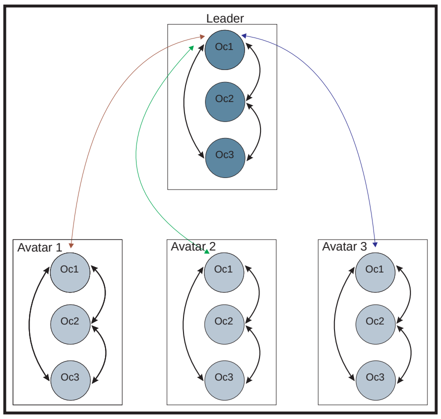

Figure 2: Coupling of multiple avatars, each of them comprising three coupled oscillators.

emotional walking (style b), the mixing weights and the mean joint angles are linearly interpolated:

$$\begin{aligned}
w_{ij}(t) &= \mu(t)\, w_{ij}^a + (1 - \mu(t))\, w_{ij}^b \\
m_i(t) &= \mu(t)\, m_i^a + (1 - \mu(t))\, m_i^b
\end{aligned} \tag{9}$$

The time-dependent morphing parameter $\mu(t)$ specifies movement style. In addition, the gait speed is adjusted by interpolating the eigenfrequencies of the oscillators:

$$\omega_0(t) = \mu(t)\, \omega_0^a + (1 - \mu(t))\, \omega_0^b \tag{10}$$

The same type of morphing was also applied to implement direction changes of the avatars for navigation, morphing between straight and curved gait steps. The change of the morphing parameter can be made dependent on the behaviour of other avatars in the scene, e.g. to influence the emotional style dependent on the distance d of the avatar from another 'dangerous' colleague, by introducing a distance-dependent morphing weight. $\mu(t) = g(d(t))$. Similarly, the eigenfrequency can be made dependent on the distance from other agents. In this way, the walking speed of a 'follower' can be adjusted to that of a leader.

4 NAVIGATION

The model so far is capable of synthesizing joint angle trajectories with high degrees of realism in real time. Yet, the characters need to change position and to propagate in the simulated scene. We compute the translated motion in the horizontal plane and the rotation of the hip around the vertical axis in order to ensure the floor contact constraints of the feet. In this way, we generate the propagation of the avatars indirectly from the joint angle movements. By interpolating between straight and curved walking we simulate walking with differently curved walking paths. Addition of a navigation dynamics makes it possible to simulate avatars that move towards specific targets in space, or to avoid obstacles and other avatars.

4.1 Character propagation

The pelvis forms the root of the kinematic chain of our avatar model. The core of the algorithm for computing the avatar's propagation is to adjust the horizontal pelvis translation and rotation in order to fulfil the constraint that the feet that make contact to the ground do not translate. For this purpose, we first detect whether the feet make ground contact using a simple threshold criterion for the vertical position of the foot centers. This criterion works well when the original motion capture data did not contain foot slipping. The correction was based on the foot with the lowest vertical coordinate.

We add a differential translation and horizontal rotation to the pelvis coordinate system in order to minimize foot slipping. In addition, the vertical position of the pelvis is adjusted by assuming that the foot forms the lowest point of the figure.

4.2 Navigation dynamics

Reactive behaviour of navigating robots and also humans has been successfully modeled using nonlinear dynamical systems [Sch95a; War06a]. We applied a simple dynamic navigation model, originally developed in robotics. The present implementation does not modify the propagation speed of the characters, while this could be easily added. The heading direction of character i is modelled by the dynamic variable $\varphi_i(t)$. The change of the heading direction is determined by three components of the vector field of the heading dynamics:

$$d\varphi_i/dt = h^{\mathrm{goal}}\left(\varphi_i, \mathbf{p}_i, \mathbf{p}_i^{\mathrm{goal}}\right) + \sum_j h^{\mathrm{avoid}}\left(\varphi_i, \mathbf{p}_i, \mathbf{p}_j\right) + \sum_j h^{\mathrm{pcoll}}\left(\varphi_i, \varphi_j, \mathbf{p}_i, \mathbf{p}_j\right) \tag{11}$$

The two-dimensional vectors $\mathbf{p}_i$ and $\mathbf{p}_j$ signify the (2D) positions of the characters i and j in the scene, and the variables $\varphi_i(t)$ and $\varphi_j(t)$ their heading directions, which can be estimated from the momentary velocities. The first term in the vector field permits to define a goal position $\mathbf{p}_i^{\mathrm{goal}}$ that the character tries to approach. It is defined by the function $h^{\mathrm{goal}}\left(\varphi_i, \mathbf{p}_i, \mathbf{p}_i^{\mathrm{goal}}\right) = \sin(\varphi_i^{\mathrm{goal}} - \varphi_i)$, where $\varphi^i_{\mathrm{goal}}$ is the direction angle of the goal relative to the position $\mathbf{p}_i$ in external coordinates.

Following [Sch95a], the second term that is responsible for obstacle avoidance is defined by:

$$h^{\mathrm{avoid}}\left(\varphi_i, \mathbf{p}_i, \mathbf{p}_j\right) = \sin\left(\Delta\varphi_{ij}\right) \cdot \exp\left(-\frac{\Delta\varphi_{ij}^2}{2\sigma_\varphi^2}\right) \cdot \exp\left(-\frac{d_{ij}^2}{2\sigma_d^2}\right) \tag{12}$$

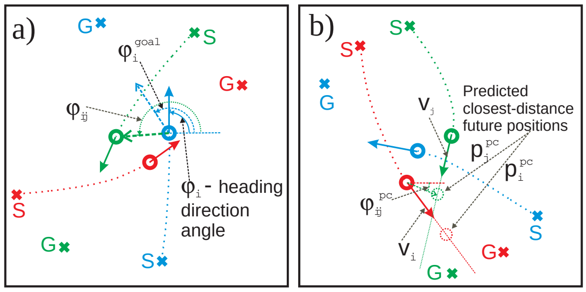

Figure 3: Avoidance scenarios illustrating the notations used in the text: (a) Angles $\varphi_i, \varphi_i^{\mathrm{goal}}, \varphi_{ij}$ shown for one character (blue). (b) Angle $\varphi_{ij}^{\mathrm{pc}}$ shown for one character (red). Crosses mark "Start" and "Goal" positions for the characters

The quantity $\Delta\varphi_{ij} = \varphi_i - \varphi_{ij}$ is the relative direction of character j seem from character i in global coordinates. Introducing the vector $\mathbf{d}_{ij} = \mathbf{p}_j - \mathbf{p}_i$ one obtains $\varphi_{ij} = \arctan((\mathbf{d}_{ij})_y/(\mathbf{d}_{ij})_x)$ and $d_{ij} = \left|\mathbf{d}_{ij}\right|$, the 2D distance between the two characters (Figure 3 a). The values of the constants were $\sigma_\varphi = \pi/6$ and $\sigma_d = 1.5\ldots2$ m. In order to remove far field interactions, we set h^{avoid} to zero for $\left|\Delta\varphi_{ij}\right| \geq \pi/2$ and for $d_{ij} > 4$ m. The last term in (11) implements an avoidance strategy that takes into account predicted possible future collision positions. Inclusion of this term provided the most naturally looking avoidance behaviour. The implemented force depends on the future positions of the characters i and j, computed from their current positions and momentary velocities $\mathbf{v}_i$, $\mathbf{v}_j$ (Figure 3 b). We define $\Delta\varphi_{ij}^{\mathrm{pc}} = \varphi_i - \varphi_{ij}^{\mathrm{pc}}$ the direction to the character j at the expected moment of minimal distance. With $\mathbf{v}_{ij} = \mathbf{v}_j - \mathbf{v}_i$ and $\mathbf{d}_{ij} = \mathbf{p}_j - \mathbf{p}_i$ the characters approach each other only for ${\mathbf{v}_{ij}}^T\mathbf{d}_{ij} < 0$. In this case, the closest relative position in the future occurs after the time $\tau^{\mathrm{pc}} = {\mathbf{v}_{ij}}^T\mathbf{d}_{ij}/({\mathbf{v}_{ij}}^T\mathbf{v}_{ij})$. At this point in time the predicted position and heading direction of character j are given by $\mathbf{p}_j^{\mathrm{pc}} = \mathbf{p}_j + \tau^{\mathrm{pc}}\mathbf{v}_j$ and $\varphi_{ij}^{\mathrm{pc}} = \arctan((\mathbf{p}_j^{\mathrm{pc}} - \mathbf{p}_i)_y/(\mathbf{p}_j^{\mathrm{pc}} - \mathbf{p}_i)_x)$, $\mathbf{d}_{ij}^{pc} = \mathbf{p}_j^{pc} - \mathbf{p}_i$. Analogous to (12), the avoidance dynamics is

$$h^{\mathrm{pcoll}}\left(\varphi_i, \varphi_j, \mathbf{p}_i, \mathbf{p}_j\right) = \sin\left(\Delta\varphi_{ij}^{\mathrm{pc}}\right) \cdot \exp\left(-\frac{(\Delta\varphi_{ij}^{\mathrm{pc}})^2}{2\sigma_\varphi^2}\right) \cdot \exp\left(-\frac{\left(d_{ij}^{\mathrm{pc}}\right)^2}{2\sigma_d^2}\right). \tag{13}$$

where the constants σ_φ and σ_d were chosen as before, and where h^{pcoll} was set to zero for $\left|\Delta\varphi_{ij}^{\mathrm{pc}}\right| \geq \pi/2$ and $d_{ij}^{\mathrm{pc}} > 8$ m.

4.3 Control of walking direction

The walking direction of the characters is changed by interpolation between straight walking and walking

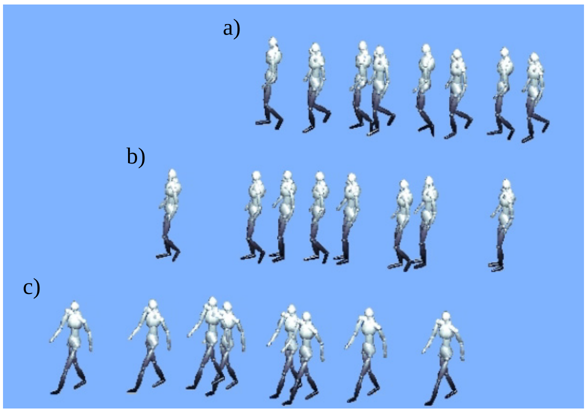

Figure 4: Synchronization of the gaits within a crowd. (a) Avatars start with self-paced walks that are out of phase. After a transitory period (b), the gaits of the characters become completely synchronized (c).

along curved paths to the left (for $\mathrm{d}\varphi_\mathrm{i}/\mathrm{dt} > 0$ or to the right ($\mathrm{d}\varphi_\mathrm{i}/\mathrm{dt} \leq 0$) using equation (9). The morph parameter μ was taken proportional to $|\mathrm{d}\varphi_\mathrm{i}/\mathrm{dt}|$, normalizing in a way that ensures $\mu = 1$ for the maximum possible value of this derivative. The heading direction $\varphi_i(t)$ generated by the navigation dynamics was low-pass filtered with a time constant equal to one step cycle to improve the smoothness of the navigation behaviour.

5 RESULTS

The proposed technique for motion capture-based self-organized simulation of character behaviour has a broad application spectrum, which could only be partially be explored in this paper. In the following, we present a number of example applications that highlight possibilities of the approach. In general the method provide very accurate approximations of the original joint trajectories, as shown in the attached *Demos*[1].

The first example shows the self-organization of coordinated behaviour of many avatars. A crowd of characters is first locomoting individually without fixed phase relationship. An instruction to move synchronously (in lock-step) is introduced, modelled by introducing couplings between the oscillator triples of the individual avatars, taking one oscillator as a leader (Section 3.3). For appropriate coupling, the transition between uncoordinated and coordinated crowd behaviour is quite short (less than three steps) and looks quite natural. After the transition, the characters adapt walking behaviour that looks highly realistic [*Demo*[2]].

The second example is shown in Figure 5. One character is following the second at a fixed distance.

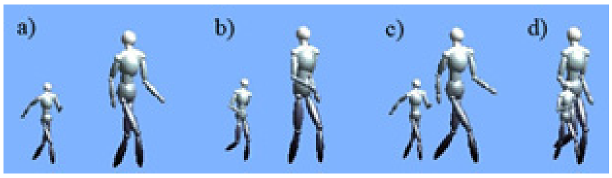

Figure 5: Following behaviour realized by two coupled avatars. (a) With the distance exceeding a certain threshold the smaller avatar accelerates (b-c) to catch up with the leader (d).

The small character has to change his eigenfrequency to catch up with the big avatar, who takes the role of the leader. This behaviour was simulated by making the eigenfrequencies of the oscillators of the follower dependent on the distance to the leader [cf. *Demo*[3]].

The third example is illustrated in Figure 6. A group of avatars that meets in the center of the scene changes their affect upon the contact with the other characters. This behaviour was implemented by making the affect of each avatar dependent on the distance from the others. In addition, the avatars avoid each other, due to the navigation dynamics described in Section 4. In this simulation, navigation and changes of emotional styles were combined, based on only three prototypical gaits: neutral walking with rotation right or left and emotional straight walking. The *Demos*[4] show examples for navigation with emotional changes from neutral to happy, neutral to sad, and sad to happy.

In order to produce the morphs between straight emotional gaits and neutral curved walking (Left and Right), we first created an intermediate balanced mixture by interpolating the mixing weights according to the relationship:

$$\begin{aligned} w_{ij} \quad = \quad & \frac{3}{4} w_{ij}^{\text{emotional}} + \\ & \frac{1}{8}\left((1+\beta_{LR}) w_{ij}^{\text{Left}} + (1-\beta_{LR}) w_{ij}^{\text{Right}}\right) \end{aligned} \tag{14}$$

Where the parameter β_{LR}, with $0 < \beta_{LR} < 1$, was adjusted for different emotional styles in order to balance left-right declinations from the straight line. Corresponding with Section 4, morphing was done in a piecewise linear manner dependent on the sign of the change of the heading direction.

Another simulation based on a similar implementation is shown in Figure 7. Here two groups of avatars cross each other, avoiding collision. When they meet each other their emotions switch to another affect. The simulation shows that the proposed framework integrates style morphing and autonomous navigation

[1] www.uni-tuebingen.de/uni/knv/arl/avi/compareA.avi
www.uni-tuebingen.de/uni/knv/arl/avi/compareS.avi
[2] www.uni-tuebingen.de/uni/knv/arl/avi/synchronization.avi

[3] www.uni-tuebingen.de/uni/knv/arl/avi/following.avi
[4] www.uni-tuebingen.de/uni/knv/arl/avi/avoidance3NH.avi
www.uni-tuebingen.de/uni/knv/arl/avi/avoidance3NS.avi
www.uni-tuebingen.de/uni/knv/arl/avi/avoidance3SH.avi

 ISBN 978-86943-15-2

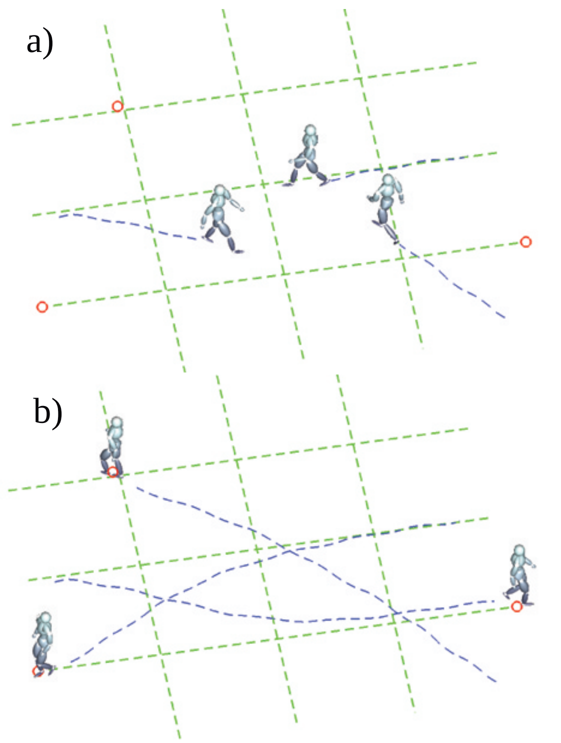

Figure 6: Avoidance behaviour and change of emotional style. a) Avatars starting from different positions with a sad emotion are heading towards their goals (red circles). b) At the meeting point the emotional styles change to happy. In addition, the characters avoid each other.

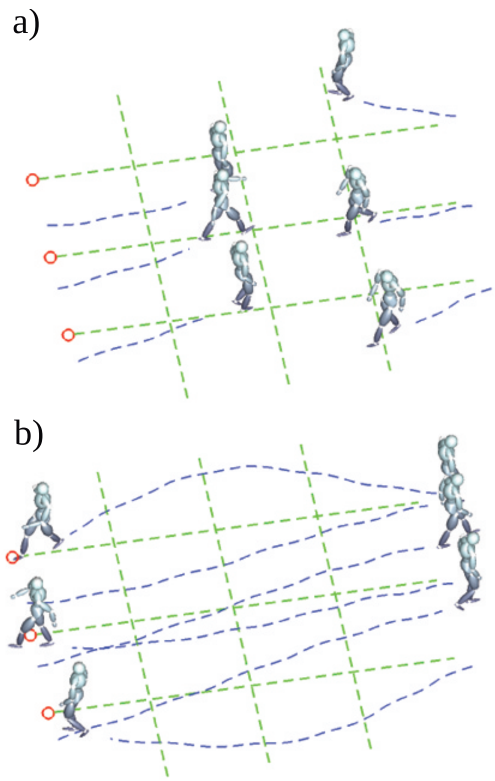

Figure 7: Avoidance behaviour and change of emotional style. Three avatars, starting from the left side, change their emotion from happy to sad while proceeding to their goals. A second group of avatars starting from the right side change their emotions from sad to happy while avoiding the opposing group.

of characters. Few examples are demonstrated *Demos*[5], including transition between neutral and emotional gaits and different emotional gaits.

6 CONCLUSION

We have presented a new framework that links the synthesis of highly realistic human movements based on motion capture data with the self-organization of behaviour using nonlinear dynamical systems. The proposed method exploits biologically inspired concepts and is based on the learning of highly compact models for human movement trajectories by a superposition of learned 'synergies', which are controlled by nonlinear attractors dynamics. By introducing of appropriate dynamic couplings complex realistically looking behaviour, reproducing the fine structure of human movements, could be synthesized.

The present paper has only given a fist set of demonstrations, and substantial additional work will be needed to explore the limits of this approach. Specifically, it needs to be demonstrated and quantified what the benefits of a synergy-based approach over other classical approaches are. The present implementation has not been optimized for computation speed and efficiency. While we tested simulations up to 20 characters, it remains to be explored how the computational limits of the proposed methods are for an appropriately chosen optimized hardware in comparison with other approaches.

Future work will extend this approach for non-periodic movements and will exploit more the synergy concept, trying to learn components that encompass only limited sets of degrees of freedom, potentially resulting in more flexible control of motion styles. An additional very interesting application field for such methods is facial animation. Here, synergies might correspond to sets of statistically optimized 'facial action units' [Ekm78a] that are adapted to the relevant animation data. In addition, such extracted statistical basis units could be compared to the classical concept of facial action units in psychology and to EMG recordings providing signatures of real physiological synergies of facial actions.

[5] www.uni-tuebingen.de/uni/knv/arl/avi/avoid6.avi
www.uni-tuebingen.de/uni/knv/arl/avi/avoid6N.avi
www.uni-tuebingen.de/uni/knv/arl/avi/avoid6NHS.avi

 ISBN 978-86943-15-2

ACKNOWLEDGEMENTS

Supported by DFG Forschergruppe 'Perceptual Graphics', Volkswagenstiftung, HFSP and EC FP6 project COBOL. Additional support was provided by the Hermann and Lilly-Schilling-Stiftung. We are grateful to T. Flash and J.J. Slotine for many interesting discussions and W. Strasser for his support.

REFERENCES

[And87a] Andronov, A.A., Vitt, A.A. and Khaikin, S.E., Theory of oscillators, Dover Publ. Inc., New York, 1987.

[Ari03a] Arikan, O., Forsyth, D.A. and O'Brien, J.F., Motion synthesis from annotations, ACM Trans. on Graph. SIGGRAPH, Vol.22, No.3, pp. 402-408, 2003.

[Ber67a] Bernstein, N.A., The coordination and regulation of movements, Pergamon Press, Oxford, 1967.

[Cha05a] Chai, J. and Hodgins, J.K., Performance Animation from Low-dimensional Control Signals, ACM Trans. on Graph. SIGGRAPH, Vol.24, No.3, pp. 686-696, 2005.

[d'Av05a] d'Avella, A. and Bizzi, E., Shared and specific Muscle synergies in neural motor behaviors, Proc. Nat. Acad. Sci. USA, Vol.102, No.8, pp. 3076-3081, 2005.

[Ekm78a] Ekman, P. and Friesen, W., Facial Action Coding System: A Technique for the Measurement of Facial Movement, Consulting Psychologists Press, Palo Alto, 1978.

[Fla05a] Flash, T. and Hochner, B., Motor primitives in vertebrates and invertebrates, Curr. Opin. Neurobiol., Vol.15, No.6, pp. 660-666, 2005.

[Gle98a] Gleicher, M., Retargetting Motion to New Characters, Proc. ACM SIGGRAPH, Int. Conf. on Comp. Graph. and Interactive Techniques, pp. 33-42, 1998.

[Gle03b] Gleicher, M., Shin, H. J., Kovar, L. and Jepsen, A., Snap-together motion: Assembling runtime animation, ACM Trans. on Graph. SIGGRAPH, Vol.22, No.3, pp. 702-702, 2003.

[Grz98a] Grzeszczuk, R., Terzopoulos, D. and Hinton, G., NeuroAnimator: Fast neural network emulation and control of physics based models, Proc. ACM SIGGRAPH, Int. Conf. on Comp. Graph. and Interactive Techniques, pp. 9-20, 1998.

[Hod95a] Hodgins, J.K., Wooten, W.L., Brogan, D.C. and O'Brien, J.F., Animating human athletics, Proc. ACM SIGGRAPH, pp. 71-78, 1995.

[Hsu05a] Hsu, E., Pulli, K. and Popović, J., Style Translation for Human Motion, ACM Trans. on Graph. SIGGRAPH, Vol.24, No.3, pp. 1082-1089, 2005.

[Ijs02a] Ijspeert, A., Nakanishi, J. and Schaal, S., Learning Attractor Landscapes for Learning Motor Primitives, In S. Becker et al eds., Adv. in Neural Inf. Process. Systems, Vol.15, pp. 1547-1554, 2002.

[Iva04a] Ivanenko, Y., Poppele, R. and Lacquaniti, F., Five basic muscle activation patterns account for muscle activity during human locomotion, Vol.556, pp. 267-282, 2004.

[Kel95a] Kelso, J.A.S., Dynamic Patterns: The Self-Organization of Brain and Behavior, MIT Press, Cambridge, 1995.

[Mat03a] Matz, G. and Hlawatsch, F., Wigner distributions (nearly) everywhere: Timefrequency analysis of signals, systems, random processes, signal spaces, and frames, Signal Processing, Vol.83, No.7, pp. 1355-1378, 2003.

[Oml07a] Omlor, L. and Giese, M.A., Extraction of spatio-temporal primitives of emotional body expressions, Neurocomp., Vol.70, pp. 10-12, 2007.

[Oml06b] Omlor, L. and Giese, M.A., Blind source separation for over-determined delayed mixtures, Adv. in Neural Inf. Process. Syst., Vol.19, pp. 1049-1056, 2006.

[Ros96a] Rose, C., Guenter, B., Bodeheimer, B. and Cohen, M.F., Efficient Generation of Motion Transitions Using Spacetime Constraints, Proc. ACM SIGGRAPH, Int. Conf. on Comp. Graph. and Interactive Techniques, Vol.30, pp. 147-154, 1996.

[Saf04a] Safanova, A., Hodgins J.K. and Pollard, N.S., Synthesizing physically realistic human motion in low-dimensional, behavior-specific spaces, Proc. ACM SIGGRAPH, Vol.23, No.3, pp. 514-521, 2004.

[Sch03a] Schaal, S., Ijspeert and A., Billard, A., Computational approaches to motor learning by imitation, Philos Trans of the R Soc of London, Biol. Sci., Vol.358, No.1431, pp. 537-547, 2003.

[Sch95a] Schöner, G., Dose, M. and Engels C., Dynamics of behavior: Theory and applications for autonomous robot architectures, Robotics and Autonomous Sys., Vol.16, No.2-4, pp. 213-245, 1995.

[Sha05a] Shao W. and Terzopoulos, D., Artificial intelligence for animation: Autonomous pedestrians, Proc. ACM SIGGRAPH, Vol.69, No.5-6, pp. 19-28, 2005.

[Ulic02a] Ulicny, B. and Thalmann, D., Towards Interactive Real-Time Crowd Behavior Simulation, Comp. Graph. Forum, Vol.21, No.4, pp. 767-775, 2002.

[Vap98a] Vapnik, V., Statistical Learning Theory, Wiley-Interscience, New York, 1998.

[Wan05a] Wang, W. and Slotine, J.J.E., On Partial Contraction Analysis for Coupled Nonlinear Oscillators, Biological Cybernetics, Vol.92, No.1, pp. 38-53, 2005.

[War06a] Warren W.H., The Dynamics of Perception and Action, Psychological Rev., Vol.113, No.2, pp. 358-389, 2006.

[Wit95a] Witkin, A. and Popović, Z., Motion warping, Proc. ACM SIGGRAPH, Annual Conf. Series, Vol.29, pp. 105-108, 1995.